755. A survey of Hopf bifurcation analysis in nonlinear railway wheelset dynamics

Hamid M. Sedighi[1], Kourosh H. Shirazi[2]
Department of Mechanical Engineering, Shahid Chamran University, Ahvaz, Iran
E-mail: [1]*hmsedighi@gmail.com*, [2]*k.shirazi@scu.ac.ir*

(Received 7 December 2011; accepted 14 February 2012)

Abstract. This article attempts to analyze the Hopf bifurcation behavior of a railway wheelset in the presence of dead-zone and yaw damper nonlinearities. A model that is more precise than Yang and Ahmadian is investigated. Using Bogoliubov-Mitropolsky averaging method and critical speed, the amplitude of the limit cycle in the presence of the mentioned nonlinearities is taken into consideration. To solve these nonlinear equations analytically, the integration interval has been divided into three sub-domains. Two-dimensional bifurcation diagrams are provided to illustrate the mechanism of formation of Hopf bifurcation. These diagrams can be used for design of stable wheelset systems.

Keywords: Hopf bifurcation, hunting, rail wheelset, discontinuous nonlinearity, analytical approach.

Introduction

High-speed railway vehicles are assuming an ever-increasing importance in today's transportation infrastructures. As the velocity of rail vehicle increases, the vehicle becomes less stable and ultimately exhibits rigorous oscillations, namely "Hunting". It has been only last two decades that analyses have been made incorporating some of the more important nonlinearities that lead to the occurrence of the hunting, such as clearances between components, the wheel flange contacting forces, dry friction in suspension components etc. Yang and Ahmadian [1] reported that De Pater [2] used Krylov and Bogoliubov [3] method to examine limit cycle behavior of a two-axle bogie with cylindrical wheels. Law and Brand [4] used the same method to analyze the dynamics of a single wheelset having curved wheel profiles and flange contact, where they modeled the effects of this flange force by a linear rail spring with a dead-band equal to the flange clearance.

The nonlinear studies led to more advanced research that used bifurcation and chaos theory in dynamic systems. Huilgol [5] first investigated the Hopf bifurcation in a wheelset, in the presence of the nonlinear contact force between the wheel and the rail. Later, Lohe and Huilgol [6] found an asymmetric oscillation in their numerical simulation. Subsequently, a group of scientists led by True Hans [7] further studied the bifurcations in two rail bogie models, where nonlinear creep force and dead-band wheel/rail contact force are considered. They found periodic, bi-periodic and chaotic behavior in this model and stated that subcritical Hopf bifurcation is popular in rail vehicles. The relationship between the damping and the critical hunting speed of a truck has been studied by Wickens [8, 9]. Chung and Shim [10] studied the Hopf bifurcation in a rail bogie. They found that introducing hysteretic nonlinearity leads to supercritical bifurcation. Pombo and Ambrósio [11] analyzed the implementation of a multi joint wheel–rail contact model to railway dynamics in small radius curved tracks. Yang and Ahmadian [12] analyzed Hopf bifurcation in a wheelset in the presence of nonlinear yaw damper in a primary suspension system.

The flange force is modeled as a linear spring besides a nonlinear fourth order damping including a dead-zone due to the wheel/rail clearance. Sedighi et al. [13-18] have modeled the dead-zone nonlinearity and other discontinuities using continuities based function to facilitate the severe computational issues that are encountered in the analytical investigations of nonlinear problems. This investigation emphasizes the influences of suspension nonlinearities and the wheel/rail interface nonlinearities on Hopf bifurcation. Frequency of the limit cycle is found

analytically. Also using the Averaging method a relation between the limit cycle amplitude and parameters of the system is introduced. These relations lead to several analytical criteria for prediction of possibility of hunting behavior. Two-dimensional bifurcation diagrams are depicted to study the Hopf bifurcation in the system.

Governing equations of motion of a single-axle wheelset

The wheelset is considered to be a 4 degrees of freedom system and is illustrated in Fig. 1.

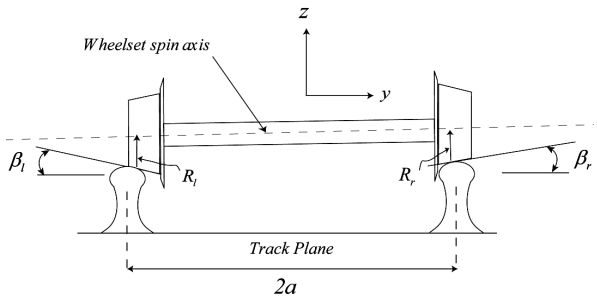

Fig. 1. Free-body diagram for wheelset

The equations of motion are organized using Newton's second law of motion for *x*, *y*, *z* and φ as follows:

$$m_w\ddot{y} = F_{ly} + F_{ry} - N_r\sin(\beta_r - \varphi) + N_l\sin(\beta_l + \varphi) + F_{s,y} - F_T \tag{1}$$

$$I_{wz}\ddot{\psi} - (I_{wx} - I_{wy})\dot{\varphi}\dot{\theta} = a(F_{rx} - F_{lx}) - a\psi[N_r\sin(\beta_r - \varphi) + N_l\sin(\beta_l + \varphi)] + M_{zr} + M_{zl} + a\psi(F_{ry} - F_{ly}) + M_{s,z} - 2bF_d \tag{2}$$

$$I_{wx}\ddot{\varphi} - (I_{wy} - I_{wz})\dot{\theta}\dot{\psi} = [N_r\sin(\beta_r - \varphi)R_r - N_l\sin(\beta_l + \varphi)R_l] + (M_{yr} + M_{yl})\psi + R_l[F_{lx}\psi - F_{ly}] + a[-N_r\cos(\beta_r - \varphi) + N_l\cos(\beta_l + \varphi)] + R_r[F_{rx}\psi - F_{ry}] + a[-F_{ry} + F_{lz}] \tag{3}$$

$$m_w\ddot{z} = F_{rz} + F_{lz} + N_r\cos(\beta_r - \varphi) + N_l\cos(\beta_l + \varphi) - m_w g \tag{4}$$

where:

$$F_{xp} = -f_{33}\xi_x,\ F_{yp} = -f_{11}\xi_y - f_{12}\xi_{sp},\quad M_{zp} = f_{12}\xi_y - f_{22}\xi_{sp} \tag{5}$$

and ξ is the Kalker's creepages, for roll, pitch and yaw rates of the left and the right contact planes. Fig. 2 provides that the suspension forces in the lateral direction, $F_{s,y}$ and the suspension moments in the vertical direction, $M_{s,z}$, acting on the wheelset:

$$F_{s,y} = -2K_y y - 2C_y\dot{y},\ M_{s,z} = -2K_x b^2\psi \tag{6}$$

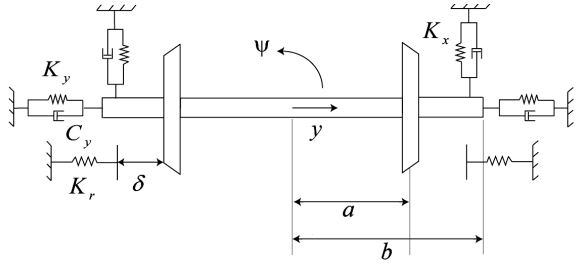

Fig. 2. The wheelset model

The nonlinear longitudinal yaw damping force F_d and the flange contact force F_T is described as follows:

$$F_d = \begin{cases} C_1 V_\psi + C_2 V_\psi^{\,2} + C_3 V_\psi^{\,3} + C_4 V_\psi^{\,4} & V_\psi > 0 \\ \\ C_1 V_\psi - C_2 V_\psi^{\,2} + C_3 V_\psi^{\,3} - C_4 V_\psi^{\,4} & V_\psi < 0 \end{cases}, \quad F_T = \begin{cases} K_r \left(y - \delta\right) & y > \delta \\ 0 & -\delta \le y \le \delta \\ K_r \left(y + \delta\right) & y < -\delta \end{cases} \tag{7}$$

where $V_\psi = b\dot{\psi}$ and the coefficients C_1 to C_4 are obtained from experimental tests on the actual dampers by [12]. The constant K_r is the wheel/rail contact lateral stiffness, and δ is the flange clearance. Assuming $\varphi = \lambda y / a$, $\dot{R} = \lambda \dot{\varphi}$, $R_l = R_r = R_0$, the vertical wheelset displacement equation of motion can be also neglected. Thus equations of motion are reduced as follows:

$$m_w \ddot{y} + m_w g \lambda \frac{y}{a} + \frac{2 f_{11}}{V}\left\{\left(1 + R_0 \frac{\lambda}{a}\right)\dot{y} - V\psi\right\} + \frac{2 f_{12}}{V}\left\{\dot{\psi} + \lambda \frac{y}{a}\frac{V}{R_0}\right\} = F_{s,y} - F_T \tag{8}$$

$$\begin{aligned} &I_{wz}\ddot{\psi} + \left(I_{wy} - I_{wx}\right)\frac{\lambda}{a}\frac{V}{R_0}\dot{y} + \frac{2 a f_{33}}{R_0}\lambda y - \frac{2 f_{12}}{V}\left\{\left(1 + R_0 \frac{\lambda}{a}\right)\dot{y} - V\psi\right\} + \frac{2 a^2 f_{33}}{V}\dot{\psi} \\ &- mg\lambda a\psi + \frac{2 f_{22}}{V}\left\{\dot{\psi} + \dot{\theta} \quad \lambda \frac{y}{a}\right\} = M_{s,z} - 2 b F_d \end{aligned} \tag{9}$$

Comparison between equation (8) with results of Yang and Ahmadian indicated that the term $\left(I_{wy} - I_{wx}\right)\frac{\lambda}{a}\frac{V}{R_0}\dot{y}$ has been omitted and the Eulerian acceleration term was deletion in their paper. As illustrated in the result section, this term changes the critical speed of the system.

Analytic behavior of the nonlinear model

Based on the achieved results for V_c and ω in the numerical simulations, the nonlinear behavior of the system can be analyzed using the Averaging method, Expanding $A(V)$ about V_c and combining equations (10) and (11) gives:

$$\dot{X} = A_0\left(V_c\right)X + \varepsilon F_1\left(X, \mu, \varepsilon\right), \quad F_1\left(X, \mu, \varepsilon\right) = BX + F\left(X\right) = \left\{0, f_2, 0, f_4\right\}^T \tag{10}$$

In which the parameters f_2, f_4 are nonlinear functions in terms of dead-zone and nonlinear yaw dampers. The eigenvectors of $A_0\left(V_c\right)$ and $A_0^{\,T}\left(V_c\right)$ corresponding to $\pm i\omega$ are $\xi_{12} = \alpha \pm i\beta$ and $\eta_{12} = p + iq$, respectively. Using the Averaging method [3], we can obtain the approximate solution of equation (10) as follows:

$$X = 2a\left(\alpha\cos\varphi - \beta\sin\varphi\right) = 2a\sqrt{\alpha^2 + \beta^2}\cos\left(\varphi + \gamma\right), \tag{11}$$

where $\gamma = tg^{-1}\left(\beta/\alpha\right)$ and the time dependent variables a and φ are defined as:

$$\frac{da}{at} = \varepsilon H_1\left(a\right), \ \frac{d\varphi}{dt} = \omega + \varepsilon G_1\left(a\right) \tag{12}$$

Using symbolic calculations, the functions $H_1(a)$ and $G_1(a)$ can be expressed as:

$$H_1(a)=\frac{1}{2\pi}\times\int_{-\gamma}^{2\pi-\gamma}\sum_{i=1}^{2} f_{2\times i}\left(p_{2\times i}\cos\varphi+q_{2\times i}\sin\varphi\right)d\varphi$$
$$G_1(a)=\frac{1}{2\pi a}\times\int_{-\gamma}^{2\pi-\gamma}\sum_{i=1}^{2} f_{2\times i}\left(q_{2\times i}\cos\varphi-p_{2\times i}\sin\varphi\right)d\varphi \tag{13}$$

The steady state solution (limit cycle) occurred if $H_1(a)=0$. Equation (13) can be used to examine the amplitude and the phase of the limit cycle. To solve for the amplitude of the stationary limit cycle, we assume:

$$H_1(a)=\frac{1}{2\pi}\int_{-\gamma}^{2\pi-\gamma}\sum_{i=1}^{2} f_{2\times i}\left(p_{2\times i}\cos\varphi+q_{2\times i}\sin\varphi\right)d\varphi=0 \tag{14}$$

which has the nontrivial solution a_1. To solve equation (14) for a_1, it is divided to three sub-domain intervals as shown in Fig. 3:

$$H_1(a)=\frac{1}{2\pi}\left(\int_{-\gamma}^{\arccos(S)-\gamma}\ldots\,d\varphi+\int_{\pi-\gamma-\arccos(S)}^{\pi-\gamma+\arccos(S)}\ldots\,d\varphi+\int_{2\pi-\arccos(S)}^{2\pi-\gamma}\ldots\,d\varphi\right) \tag{15}$$

where the term S in the integral domain is $\delta/2a\sqrt{\alpha^2+\beta^2}$. To solve for the frequency of the limit cycle, we obtained a_1 from (14) and substituted in (13):

$$\Omega=\omega+\frac{\varepsilon}{2\pi a}\int_{-\gamma}^{2\pi-\gamma}\sum_{i=1}^{2} f_{2\times i}\left(q_{2\times i}\cos\varphi-p_{2\times i}\sin\varphi\right)d\varphi \tag{16}$$

therefore the long-term behavior of the system can be obtained by substituting solution equation (14) for a into equation (11) that is given as follows:

$$X=2a_1\sqrt{\alpha^2+\beta^2}\cos\left(\Omega t+\theta+\gamma\right) \tag{17}$$

where $\vartheta=tg^{-1}\left(\alpha_1/\beta_1\right)$, the theoretical as well as the numerical simulation limit cycle are indicated in Fig. 4. This figure confirms the soundness and effectiveness of the introduced EFs.

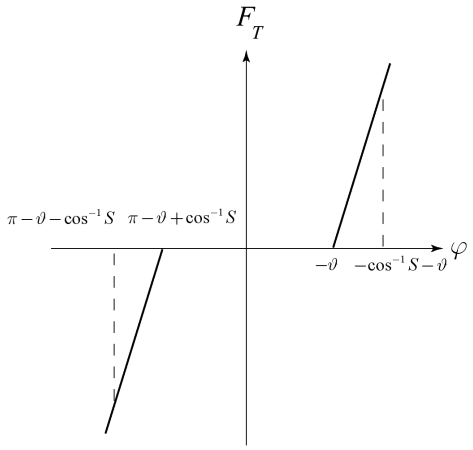

Fig. 3. Discretization of lateral contact force for analytical approach

Results

In order to analyze the influence of the system parameters on the hunting behavior, we solve equations (8) and (9) numerically. By varying forward speed V and plot stable response of the lateral displacement vs. speed, bifurcation diagrams generate as shown in Figs. 5-11. In Fig. 5 the direct numerical solution of equation of motion is depicted. As this figure indicates the V_c from numerical solution is 160 km/h.

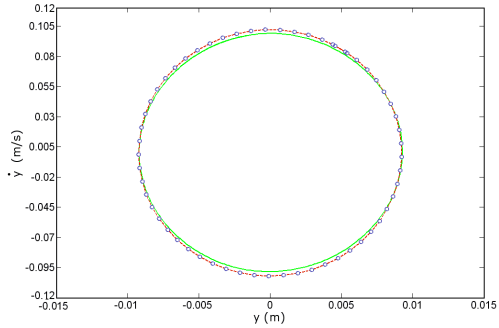

Fig. 4. Comparison of theoretical (symbols) and numerical simulation (continues line) limit cycles

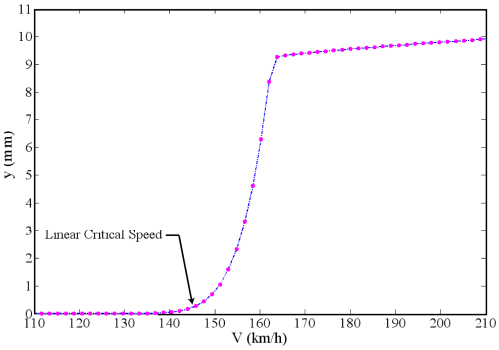

Fig. 5. Bifurcation diagram for set of main parameters

The effect of the rail stiffness (K_r) on the critical speed is considered. Fig. 6 shows that the rail stiffness has no remarkable effect on hunting speed, however it reduces hunting amplitude. Also, Fig. 7 indicates that smaller flange clearance reduces the amplitude of limit cycle with no significant effects on critical speed.

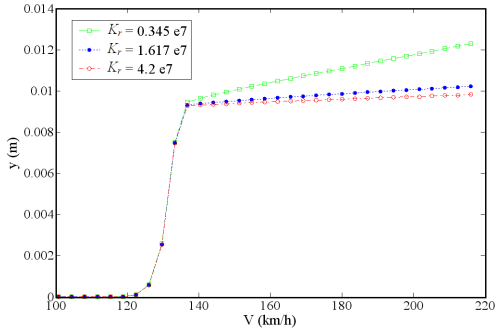

Fig. 6. The effect of rail lateral stiffness on critical speed

Through Fig. 8 to Fig. 11, the effect of variation of the parameters C_y, K_y, K_x and λ on critical speed are indicated. Increasing lateral stiffness as well as lateral damping and yaw stiffness, raises the critical speed V_c and lowers the hunting amplitude. Comparing Fig. 8 to Fig. 10 it is observed that the hunting speed shows more sensitivity to change of the yaw stiffness relative to the other parameters such as the lateral damping.

As Fig. 11 indicates increasing wheelset conicity, decreases the critical speed V_c and increases the hunting amplitude, while the hunting speed and amplitude shows more sensitivity to change of the wheelset conicity.

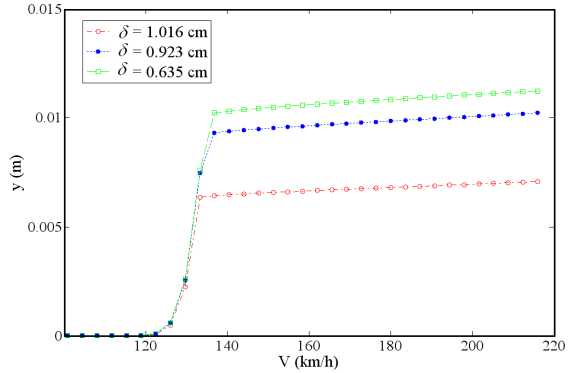

Fig. 7. The effect of flange clearance on critical speed

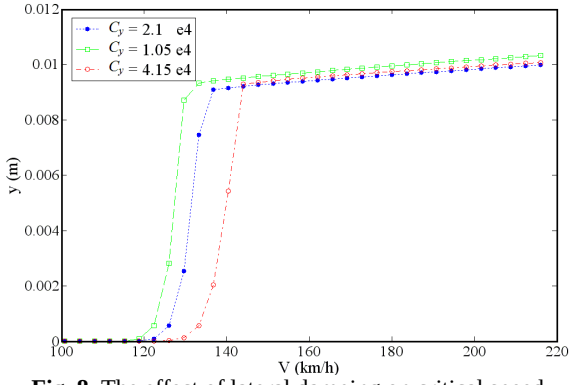

Fig. 8. The effect of lateral damping on critical speed

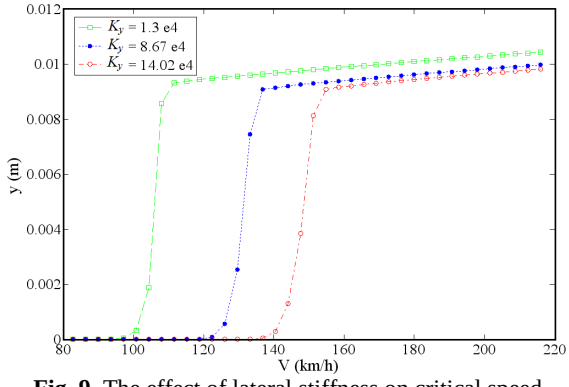

Fig. 9. The effect of lateral stiffness on critical speed

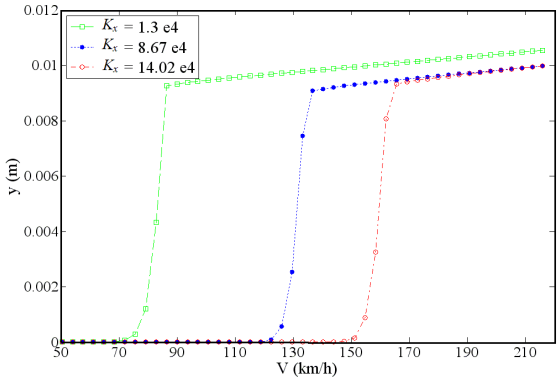

Fig. 10. The effect of yaw spring stiffness on critical speed

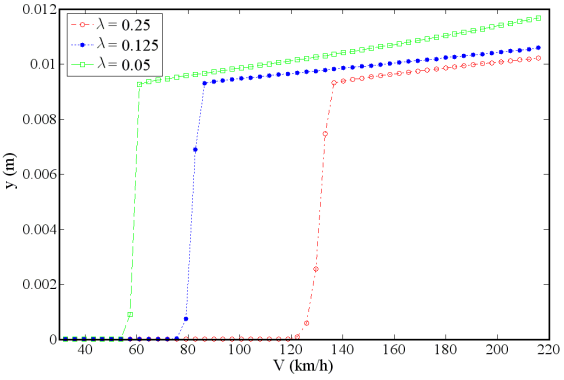

Fig. 11. The effect of wheelset conicity on critical speed

Conclusions

In this paper Hopf bifurcation in a railway wheelset was studied through a nonlinear model. Novel procedure for modeling of discontinuous nonlinearities has been employed to predict analytical response of nonlinear vibration in the time domain. It appears from the present work that the method can significantly alleviate the analytical investigation of the nonlinear problems. The authors believe that the introduced procedure has special potential to be applied to other strong nonlinearities such as preload, dead-zone and saturation discontinuous. Additionally, the effects of suspension parameters such as lateral damping and stiffness, yaw stiffness and wheelset conicity on critical speed were also investigated. The results of the investigation demonstrate that:

1. Increasing gauge clearance reduces the amplitude of hunting. Gauge clearance does not have a significant effect on the critical speed.
2. Yaw stiffness has a major effect on hunting velocity and can be an important design parameter, while increasing lateral damping has less effect on increase of the critical speed.
3. Increasing rail lateral stiffness does not significantly affect the critical speed, but reduces hunting amplitude.

References

[1] **Yang S., Chen E.** The Hopf bifurcation in a railway bogie with hysteretic nonlinearity. Journal of the China Railway Society, Vol. 15, 1993, p. 441-453.

[2] **Pater D.** The approximate determination of the hunting movement of a railway vehicle by aid of the method of Krylov and Bogoliubov. Applied Scientific Research, Vol. 9, 1960, p. 205-228.

[3] **Bogoliubov N. N., Mitropolsky Y.** Asymptotic Method in the Theory of Nonlinear Oscillations. Delhi, India: Hindustan Publishing Corp, 1961, p. 158-192.

[4] **Law E. H., Brand R. S.** Analysis of the nonlinear dynamics of a railway vehicle wheelset. Dynamic Systems, Measurement and Control, Vol. 95**,** 1973, p. 28-35.

[5] **Huilgol R. R.** Hopf-Friedrichs bifurcation and the hunting of a railway axle. PMM Journal of Applied Mathematics and Mechanics, Vol. 12, 1978, p. 85-94.

[6] **Lohe M. A., Huilgol R. R.** Flange force effects on the motion of train wheelset. Vehicle System Dynamics, Vol. 11, 1982, p. 283-303.

[7] **True H., Kaas-Petersen C.** A bifurcation analysis of nonlinear oscillations in railway vehicles. The Dynamics of Vehicles on Road and on Tracks, 8th IAVSD Symp., 1984, p. 438-444.

[8] **Wickens A. H.** The hunting stability of railway vehicle wheelsets and bogies having profiled wheels. International Journal of Solids and Structures, Vol. 1, 1965, p. 319-341.

[9] **Wickens A. H.** Static and dynamic instabilities of bogie railway vehicles with linkage steered wheelsets. Vehicle System Dynamics, Vol. 26, 1996, p. 1-16.

[10] **Chung W. J., Shim J. K.** Influence factors on critical speed hysteresis in railway vehicles. Japan Society Mechanical Engineering International Journal, Vol. 46, 2003, p. 278-288.

[11] **Pombo J. C., Ambrósio J. C.** Application of a wheel-rail contact model to railway dynamics in small radius curved tracks. Multibody System Dynamics, Vol. 19, 2008, p. 91-114.

[12] **Yang S., Ahmadian M.** The Hopf bifurcation in a rail wheelset with nonlinear damping. Proc. of Transportation Division, International Mechanical Engineering Congress and Exposition, Atlanta, 1996, p. 112-135.

[13] **Sedighi H. M., Shirazi K. H., Zare J.** Novel equivalent function for deadzone nonlinearity: applied to analytical solution of beam vibration using He's parameter expanding method. Latin American Journal of Solids and Structures, 2012, in press.

[14] **Sedighi H. M., Shirazi K. H., Reza A., Zare J.** Accurate modeling of preload discontinuity in the analytical approach of the nonlinear free vibration of beams. Proceedings of the Institution of Mechanical Engineers, Part C: Journal of Mechanical Engineering Science, 2012, doi: 10.1177/0954406211435196.

[15] **Sedighi H. M., Reza A., Zare J.** Dynamic analysis of preload nonlinearity in nonlinear beam vibration. Journal of Vibroengineering, Vol. 13, 2011, p. 778-787.

[16] **Sedighi H. M., Reza A., Zare J.** Study on the frequency – amplitude relation of beam vibration. International Journal of the Physical Sciences, Vol. 6, 2011, p. 8051-8056, doi: 10.5897/IJPS11.1556.

[17] **Sedighi H. M., Shirazi K. H.** A new approach to analytical solution of cantilever beam vibration with nonlinear boundary condition. ASME Journal of Computational and Nonlinear Dynamics, 2012, doi: 10.1115/1.4005924.

[18] **Sedighi H. M., Shirazi K. H., Noghrehabadi A. R., Yildirim A.** Asymptotic investigation of buckled beam nonlinear vibration. Iranian Journal of Science and Technology, Transaction B. Engineering, 2012, in press.